Stem Cell Reports

Article

Substance P/neurokinin-1 receptor pathway blockade ameliorates limbal stem cell deficiency by modulating mTOR pathway and preventing cell senescence

Romina Lasagni Vitar,[1] Francesca Triani,[1] Marco Barbariga,[1] Philippe Fonteyne,[1] Paolo Rama,[1] and Giulio Ferrari[1,*]

[1]Cornea and Ocular Surface Disease Unit, Eye Repair Lab, IRCCS San Raffaele Scientific Institute, Via Olgettina 60, 20132 Milan, Italy
*Correspondence: ferrari.giulio@hsr.it
https://doi.org/10.1016/j.stemcr.2022.02.012

SUMMARY

Severe ocular surface diseases can lead to limbal stem cell deficiency (LSCD), which is accompanied by defective healing. We aimed to evaluate the role of the substance P (SP)/neurokinin-1 receptor (NK1R) pathway in corneal epithelium wound healing in a pre-clinical model of LSCD. SP ablation or NK1R blockade significantly increased epithelial wound healing ($p < 0.001$) and corneal transparency ($p < 0.001$), compared with wild type (WT). In addition, a reduced number of infiltrating goblet and conjunctival cells ($p < 0.05$) and increased number of epithelial stem cells ($p < 0.01$), which also expressed NK1R, was observed. The mammalian target of rapamycin (mTOR) pathway was significantly inhibited ($p < 0.05$) and expression of γH2AX was significantly reduced ($p < 0.05$) after SP ablation. These results suggest that excessive expression of SP is associated with LSCD and results in accelerated senescence and exhaustion of residual stem cells. Topical treatment with NK1R antagonist ameliorates clinical signs associated with LSCD and could be used as an adjuvant treatment in LSCD.

INTRODUCTION

Constant renewal of the corneal epithelium is necessary to preserve corneal integrity and proper vision. Corneal nerves contribute to this process by releasing neuropeptides with trophic functions. Among them, substance P (SP) is an 11-amino-acid polypeptide that is produced from a precursor encoded by the pre-protachykinin A (TAC1) gene. Following nerve stimulation, SP is released mainly by nerve fibers (Shaheen et al., 2014), but also by immune (Mashaghi et al., 2016) and epithelial cells (Watanabe et al., 2002) in the cornea. SP mainly binds to neurokinin-1 receptor (NK1R), which is highly expressed in the cornea (Lasagni Vitar et al., 2021). Its activation is deeply implicated in the promotion of the inflammatory response as it favors corneal neovascularization and wound healing (Barbariga et al., 2018a; Bignami et al., 2014, 2017; Suvas, 2017). Existing data, however, suggest a dual role for SP. On one hand, it promotes closure of epithelial wounds (Nagano et al., 2003; Nakamura et al., 1997; Yang et al., 2014) and maintenance of normal nerve morphology (Muñoz and Coveñas, 2014). On the other, its expression directly correlates with the severity of ocular surface inflammation in patients (Barbariga et al., 2018a). While it is unclear whether the increased SP levels represent a compensatory mechanism, it is known that SP promotes leukocyte chemotaxis and extravasation, which, uncontrolled, can impair wound healing.

Corneal epithelial wounds are a common occurrence in an eye clinic. Prompt closure of these wounds is vital to preserve vision and relies on the capacity of proliferation, differentiation, and migration of limbal stem cells (Amitai-Lange et al., 2015; Di Girolamo et al., 2015; West,

2015). Different molecular pathways are involved in these processes (Ljubimov and Saghizadeh, 2015). The mammalian target of rapamycin (mTOR) signaling has been identified as a key driver of stem cell activity (Russell et al., 2011) and, recently, this pathway was reported to participate in corneal epithelial cell proliferation and differentiation (Gidfar et al., 2017; Wang et al., 2020).

Severe ocular surface diseases can lead to limbal stem cell deficiency (LSCD), which is accompanied by defective healing and ocular surface instability (Hatch and Dana, 2009). While epithelial stem cells can be transplanted (Rama et al., 2017), this treatment is not universally available and its success rate varies depending on the techniques used (Baylis et al., 2011; Sangwan et al., 2011). Autologous limbal stem cell transplantation is highly successful, but impossible in cases of complete bilateral stem cell deficiency. In these cases, allogeneic transplantation has been proposed. However, long-term survival of the graft has been questioned, and complications associated with life-long systemic immunosuppression are of concern (Atallah et al., 2016; Rama et al., 2017; Sacchetti et al., 2018). In summary, LSCD is an area of unmet medical need and causes permanent vision loss. The aim of this study was to evaluate the effects of the SP/NK1R pathway on epithelial wound healing in a pre-clinical model of corneal stem cell deficiency.
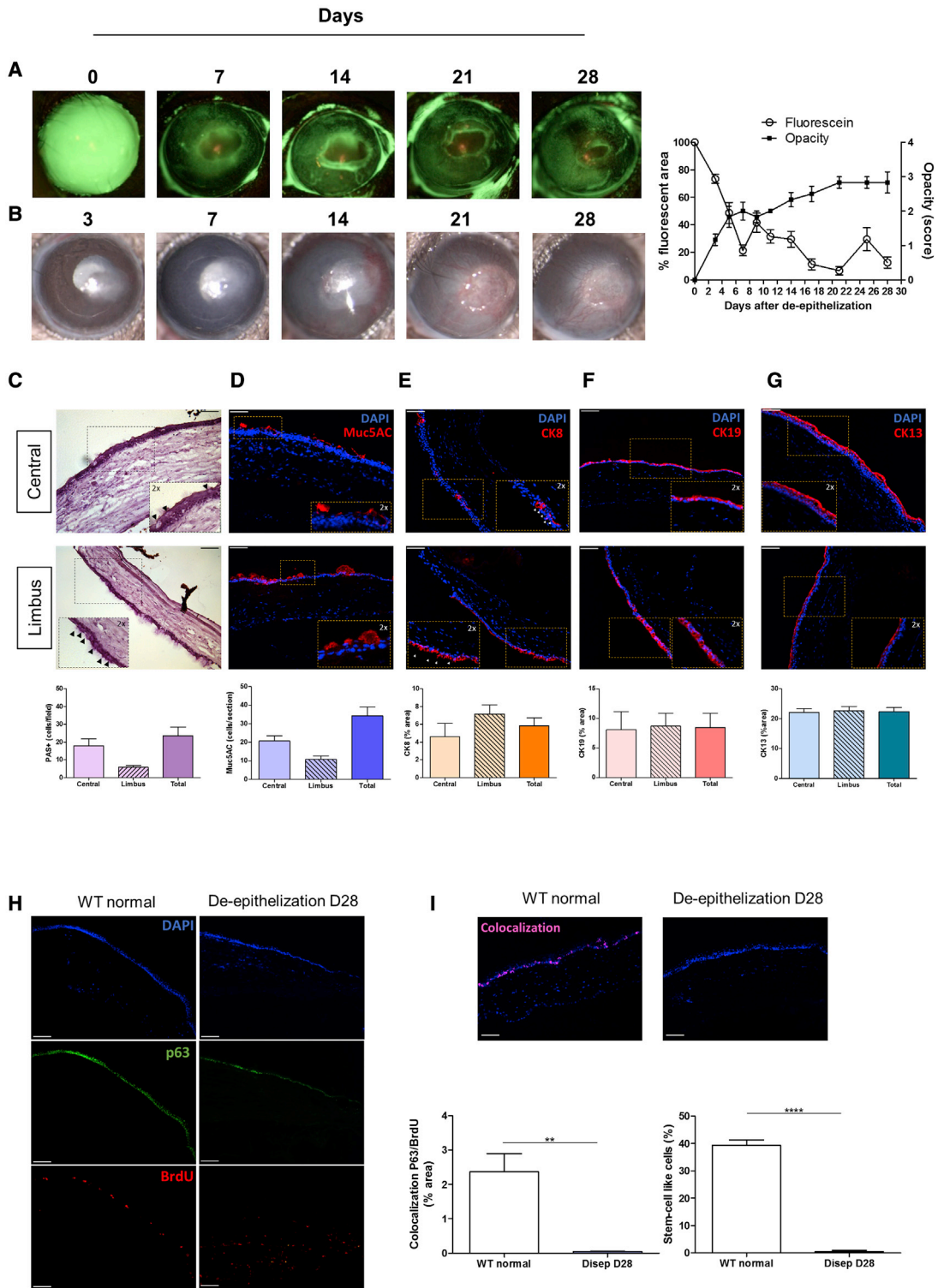
RESULTS

Corneal de-epithelization model generates a severe and stable stem cell deficiency

After 4 weeks, fluorescein staining was observed as diffuse punctate staining (Figure 1A). In addition, corneal opacity

Stem cell deficiency model stability

Days

A

0   7   14   21   28

B

3   7   14   21   28

C   D   E   F   G

Central

Limbus

H   WT normal   De-epithelization D28   I   WT normal   De-epithelization D28

(legend on next page)

and central neovascularization were observed (Figure 1B). All these features are consistent with a clinical pattern of corneal conjunctivalization due to LSCD. To confirm the conjunctivalization, we performed immunostaining to identify the presence of conjunctival goblet (periodic acid Schiff [PAS]+, Muc5AC+, and CK8+) and epithelial (CK19+ and CK13+) cells in the cornea, as shown in Figures 1C–1G. Goblet and conjunctival epithelial cells were found in both limbus and central areas of the cornea. Of note, immediately after the LSCD model was performed, we stained for corneal and conjunctival epithelial cell markers (CK12 and CK19, respectively), which were absent in both limbus and central cornea (Figure S1A). However, we identified that a low amount of p63+ CK12− cells remained in the limbus area after the procedure (5.2 ± 1.3) (Figure S1B), suggesting that a very low amount of cells with a potential proliferative capacity is left.

Finally, using the widely accepted slow-cycling characteristic of stem cells, we identified corneal epithelial stem cells using 5-bromo-2′-oxyuridine (BrdU) (Cotsarelis et al., 1989; Li et al., 2017; Pajoohesh-Ganji et al., 2012; Sartaj et al., 2017) in addition to the well-recognized stem cell marker p63 (Pellegrini et al., 2001). We found that a very low amount of stem cell-like cells remained 4 weeks after the stem cell deficiency model was performed (Figures 1H and 1I).

Altogether, we conclude that, based on the clinical parameters (punctate staining, opacity, and neovascularization), the extent of corneal conjunctivalization, and the low amount of remaining stem cell-like cells, our experimental model is stable and generates a severe LSCD.

SP ablation and NK1R blockade improves corneal epithelial wound healing and corneal transparency

After de-epithelization, *in vivo* corneal photographs were taken every day in order to evaluate wound healing progress and corneal opacity in wild-type (WT and TAC1-KO mice (Figure 2). Compared with WT, TAC1-KO mice showed significantly faster epithelial wound healing, starting from the third day after de-epithelization. By day 14, wound healing was 57% higher in TAC1-KO mice (p < 0.001), as shown by the reduced fluorescein staining (Figure 2A). Of note, when a central less severe wound was performed, both WT and TAC1-KO mice showed a wound closure of 100% by day seven (Figure S2), suggesting that SP is at play in a stem cell deficiency setting.

Additionally, TAC1-KO mice presented a significant increase in corneal transparency compared with WT mice (Figure 2B). By day 14, corneal transparency was 70% higher in TAC1-KO mice than in WT (p < 0.001).

In order to test if SP was acting through NK1R binding, we used the selective NK1R antagonist fosaprepitant in two different concentrations: 0.1 mg/mL (FOSA 0.1) and 1 mg/mL (FOSA 1). When wound healing rate was evaluated, we found that FOSA 1 mice showed a significant improvement in wound closure rate from day five compared with WT mice (p < 0.05) (Figure 3A). In addition, with FOSA 1 treatment, a better corneal transparency was achieved (p < 0.05) (Figure 3B). Mice treated with FOSA 1 showed no improvement in wound closure or corneal opacity compared with WT mice. These results suggest that SP-NK1R binding is detrimental for epithelial wound closure and corneal transparency in stem cell deficiency.

Figure 1. Corneal de-epithelization model generates a severe and stable stem cell deficiency
(A) De-epithelization was performed using a blunt spatula to scrap the entire corneal epithelium, including the limbus. Wound healing progress evaluated by fluorescein assay in wild-type (WT; n = 5) mice from day 0 until day 28.
(B) Corneal opacity evaluation using a grading score (from 0 to 4; 0 = completely clear, 4 = completely opaque).
(C) PAS staining for goblet cell identification in the cornea. Representative images are shown (40×).Scale bar, 50 μm. Quantification of PAS+ cells was performed in the limbus and central cornea.
(D) Mucin 5AC (Muc5AC) staining for goblet cell identification. Representative images are shown (20×). Scale bar, 75 μm. Quantification of Muc5AC+ cells was performed in the limbus and central cornea.
(E) Cytokeratin 8 (CK8) staining for conjunctival cell identification. Representative images are shown (20×). Scale bar, 75 μm. Quantification of CK8+ cells was performed in the limbus and central cornea.
(F) Cytokeratin 19 (CK19) staining for conjunctival cells. Representative images are shown (20×). Scale bar, 75 μm. Quantification of CK19+ cells was performed in the limbus and central cornea.
(G) Cytokeratin 13 (CK13) staining for conjunctival cells. Representative images are shown (20×). Scale bar, 75 μm. Quantification of CK13+ cells was performed in the limbus and central cornea.
(H) p63 and BrdU staining for stem cell identification. Immediately after corneal dispepithelization, animals were intraperitoneally injected with BrdU (50 μg/g body weight) twice a day (9 a.m. and 4 p.m.) for 7 days, followed by a chase period of 22 days. Representative pictures are shown (20×). Scale bar, 75 μm.
(I) Colocalization between p63 and BrdU was performed. Representative pictures of colocalization points are shown in magenta (20×). Scale bar, 75 μm. Stem cell-like cells were identified when the colocalized points represented more than 50% of the nucleus, using DAPI as a reference. Quantification was assessed in the entire corneal epithelium (limbus and central). Graphs show mean values ±SEM. Statistical analysis by one-way ANOVA followed by Tukey's test or by unpaired Student's t test: **p < 0.01, ****p < 0.0001.
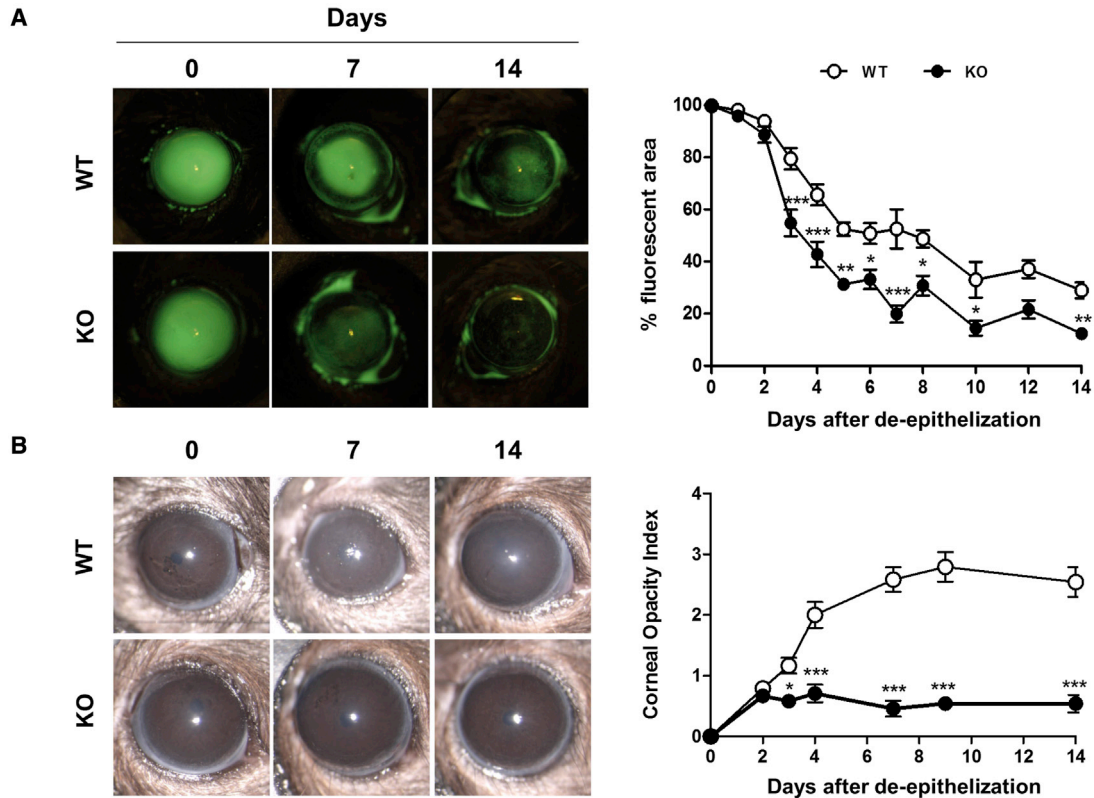
Figure 2. SP ablation improves corneal epithelial wound healing and corneal transparency in a stem cell deficiency model
(A) Stem cell deficiency model. Wound healing progress evaluated by fluorescein assay in WT (n = 10) and TAC1-KO (KO, n = 18) mice.
(B) Corneal opacity evaluation using a grading score (from 0 to 4; 0 = completely clear, 4 = completely opaque) in WT and TAC1-KO mice.
Graphs show mean values ±SEM; statistical analysis by two-way ANOVA:*$p < 0.05$, **$p < 0.01$, ***$p < 0.001$.

Goblet and conjunctival cells infiltrating the cornea are reduced in the absence of SP or by blocking NK1R

PAS staining was employed to identify goblet cells in the cornea (Ferrari et al., 2013). Representative images (40×) are shown in Figure 4A. TAC1-KO and FOSA 1 mice corneas presented a decrease of PAS$^+$ cells compared with WT ($p < 0.05$). Similarly, Muc5AC staining showed a reduced number of goblet cells in TAC-KO ($p < 0.05$) and FOSA 1 mice ($p < 0.001$) compared with the WT group (Figure 4B).

To evaluate conjunctival cells infiltrating the cornea, CK8, CK19, and CK13 staining was performed. In addition, CK12 was used to stain the corneal epithelium. Representative images (20×) of the immuno-fluorescence are shown in Figures 4C–4E. Compared with WT, TAC1-KO and FOSA 1 mice showed a reduction in CK8 ($p < 0.05$ and $p < 0.01$), CK19 ($p < 0.001$ and $p < 0.05$), and CK13 ($p < 0.01$) conjunctival cells with an increase in CK12 expression ($p < 0.001$). These results suggest that, in stem cell deficiency, SP promotes conjunctival migration into the cornea by binding to NK1R.

SP ablation and NK1R blockade alleviate stem cell deficiency

We found that both TAC1-KO and FOSA 1 mice presented an increase in BrdU staining, compared with WT ($p < 0.01$), while no differences were found in p63 content (Figure 5A). We then assessed the colocalization of the two makers and both groups displayed higher percentage of p63/BrdU co-localization ($p < 0.05$), which was located mostly in the basal epithelium (Figure 5B). Finally, we identified and quantified stem cell-like cells as the cells presenting more than 50% of the nucleus positive for both p63 and BrdU. In line with the previous results, we found that TAC1-KO and FOSA 1 mice also exhibited an increased number of stem cell-like cells ($p < 0.01$) compared with WT (Figure 5B). In addition, we also quantified the expression of ATP-binding cassette sub-family B member 5 (ABCB5), recently described as another putative marker of epithelial stem cells (Ksander et al., 2014). TAC1-KO mice exhibited an increase in ABCB5 expression in the corneal epithelium (19%, $p < 0.05$) (Figure S3).

We then evaluated whether corneal epithelial stem cells also expressed NK1R, as has been already demonstrated
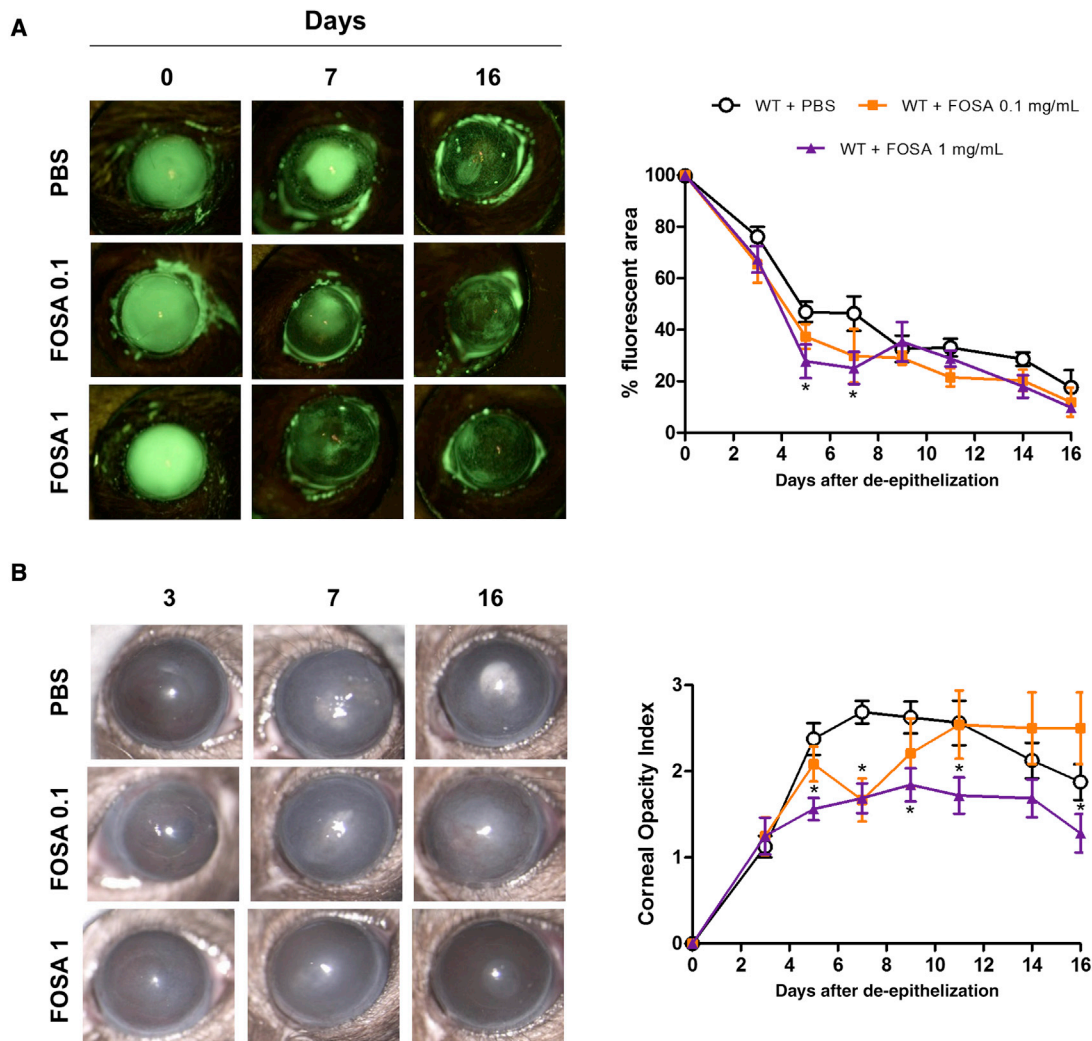
Figure 3. Neurokinin-1 receptor blockade promotes epithelial wound healing and corneal transparency in a stem cell deficiency model

(A) Wound healing progress evaluated by fluorescein assay in WT mice treated with vehicle (PBS, n = 5) and fosaprepitant 0.1 mg/mL (FOSA 0.1, n = 5) or 1 mg/mL (FOSA 1, n = 5), four times a day for 16 days.

(B) Corneal opacity evaluation using a grading score (from 0 to 4; 0 = completely clear, 4 = completely opaque) in PBS, FOSA 0.1, and FOSA 1 groups. Graphs show mean values ±SEM; statistical analysis by one-way ANOVA followed by Tukey's test: *p < 0.05.

in corneal epithelial cells (Watanabe et al., 2002). As shown in Figure 5C, corneal epithelial stem cells are also NK1R positive. Altogether, these results suggest that, after a severe wound, stem cells are preserved in the absence of SP or after blocking NK1R.

SP ablation results in decreased mTOR signaling and senescence in corneal epithelium

The ribosomal protein S6 kinase is a well-known downstream target of mTOR related to cell growth, and its phosphorylation has been used as a hallmark of mTOR pathway activation (Magnuson et al., 2012). The expression of P70S6 and pP70S6 was evaluated by western blot.

A representative blot is shown in Figure 6A. Bands of approximately 70 and 40 kDa correspond to pP70S6 or P70S6 and β-actin, respectively. Compared with WT, TAC1-KO mice showed a significant decrease in pP70S6 expression (51%, respectively, p < 0.05). A ratio between pP70S6 and P70S6 expression was performed in order to determine mTOR pathway activation. A decrease in this ratio was observed in TAC1-KO mice, compared with WT, suggesting an inhibition of the mTOR signaling pathway.

Finally, γH2AX expression was assayed as a senescence marker and as a target downregulated by the mTOR pathway. A representative blot is shown in Figure 6B. Bands of approximately 15 and 40 kDa correspond to
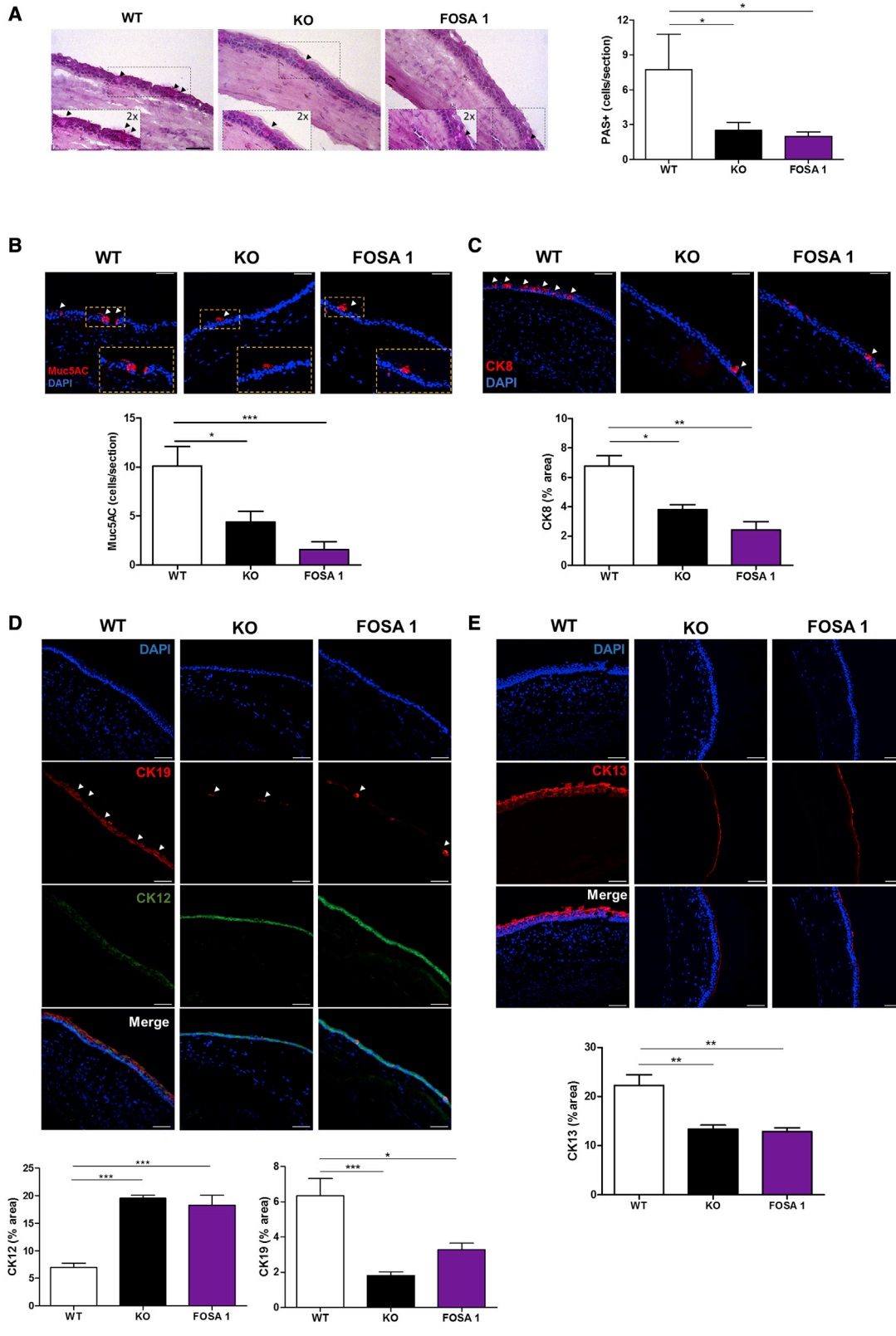
(legend on next page)

γH2AX and β-actin, respectively. TAC1-KO mice displayed a decreased γH2AX expression in comparison with WT (53%, $p < 0.05$), suggesting that cell senescence is prevented when SP is ablated.

DISCUSSION

Epithelial stem cells are indispensable to repopulate the cornea after injury and to prevent vision loss (Daniels et al., 2006; Dua and Azuara-Blanco, 2000; Dua et al., 2000). Many ocular diseases, including corneal burns, severe dry eye, and autoimmune disorders, can induce LSCD (Ahmad, 2012; Daniels et al., 2001; Hatch and Dana, 2009). In this paper, we report the beneficial effect of SP ablation or pharmacological inhibition on wound healing efficiency in a mouse model of LSCD. We found that activation of the SP/NK1R pathway promotes corneal opacity, conjunctival/goblet cell infiltration, and stem cell exhaustion. Specifically, SP aggravates corneal LSCD through stimulation of the mTOR pathway, eventually leading to accelerated corneal epithelial cell senescence. In addition, we showed for the first time that mouse corneal epithelial stem cells express NK1R and, hence, can be directly influenced by SP, as was shown in other tissues, such as the bone marrow (Li et al., 2020; Nowicki et al., 2007). Interestingly, it was suggested that the effect of SP on bone marrow stem cells is concentration dependent: while a low and controlled release of SP can stimulate stem cell proliferation, higher levels of SP are associated with detrimental effects such as malignant hematopoiesis (Nowicki et al., 2007).

It is a well-known fact that inflammation can induce depletion of stem cells in the bone marrow (King and Goodell, 2011), brain (Glass et al., 2010; Pluchino et al., 2008), and hair follicles (Doles et al., 2012), among other tissues (Kizil et al., 2015). In fact, severe and/or chronic inflammation of the ocular surface invariably accompanies LSCD in humans (Dua et al., 2000), which is why these patients require long-term topical or systemic anti-inflammatory treatments (e.g., corticosteroids). In this vein, recalcitrant ocular surface inflammation is the most common cause of autologous corneal epithelial stem cell transplantation failure (Rama et al., 2010), which suggests that inflammation can not only induce LSCD but also interfere with engraftment of transplanted stem cells. SP is a potent pro-inflammatory molecule that promotes neovascularization (Bignami et al., 2017; Ziche et al., 1990), leukocyte recruitment (Lasagni Vitar et al., 2021), and oxidative burst (Mashaghi et al., 2016; Suvas, 2017) in the cornea by binding to NK1R, although its role in LSCD remained elusive.

In order to test the effect of SP on stem cell function, we used a well-established animal model of LSCD (Amirjamshidi et al., 2011; Meyer-Blazejewska et al., 2011; Pal-Ghosh et al., 2008). This is generated through mechanical removal of corneal epithelium, including the limbus. Of note, immediately after de-epithelization, we found that a very low amount of cells with a potential proliferative capacity is left, suggesting that our model is a severe model of LSCD, but does not immediately produce a total depletion of stem cells. We confirmed that our model is stable since LSCD is maintained over time, as shown by persistent corneal epitheliopathy, opacity, neovascularization, and the very low amount of residual stem cell-like cells. Interestingly, we found that SP ablation or pharmacological inhibition of NK1R by means of fosaprepitant improved clinical outcomes such as the time for epithelial wound closure, conjunctivalization, and corneal opacity.

Multiple markers of epithelial stem cells in the mouse cornea have been described, although a definitive consensus has not been reached yet (Guo et al., 2018). Among them, BrdU-based pulse-chase experiments have been extensively used to identify corneal stem cells due to their slow-cycling nature (Cotsarelis et al., 1989; Li et al., 2017; Pajoohesh-Ganji et al., 2012; Park et al., 2019; Sartaj et al., 2017). Furthermore, it has been shown

Figure 4. SP ablation or neurokinin-1 receptor blockade reduces the number of goblet and conjunctival cells infiltrating the cornea
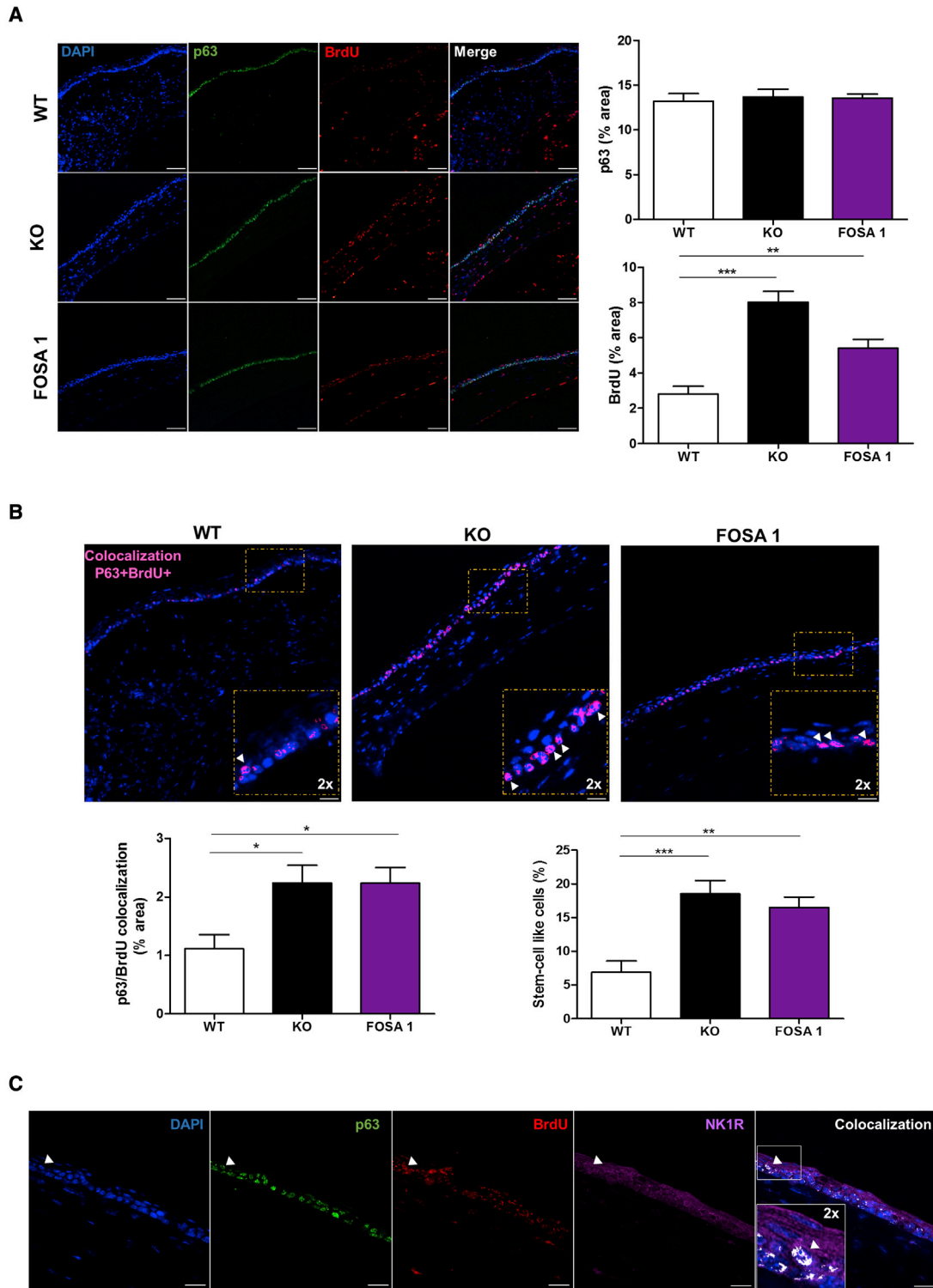
(A) PAS staining for goblet cell identification in the cornea. Representative images are shown (40×). Scale bar, 50 μm. Quantification was performed along the entire cornea (limbus and central).

(B) Muc5AC staining for goblet cell identification. Representative images are shown (20×). Scale bar, 75 μm. Quantification of Muc5AC^{+} cells was performed in the limbus and central cornea.

(C) CK8 staining for conjunctival cell identification. Representative images of the immunofluorescence are shown (20×). Scale bar, 75 μm. Quantification was performed along the entire cornea (limbus and central).

(D) Cytokeratin 12 (CK12) and CK19 staining for corneal and conjunctival cells, respectively. Representative images are shown (20×). Scale bar, 75 μm. The last figure of the panel represents the merge between DAPI, CK12, and CK19. Quantification was performed along the entire cornea (limbus and central).

(E) CK13 staining for conjunctival cells. Representative images are shown (20×). Scale bar, 75 μm. Quantification was performed along the entire cornea (limbus and central). Graphs show mean values ±SEM (n = 5 mice/group); statistical analysis by one-way ANOVA followed by Tukey's test: *$p < 0.05$, **$p < 0.01$, ***$p < 0.001$.

Figure 5. SP ablation or neurokinin-1 receptor blockade alleviates stem cell deficiency

Neurokinin-1 receptor is expressed by corneal stem cell-like cells.

(A) p63 and BrdU staining for stem cell identification. Immediately after corneal dispepithelization, animals were intraperitoneally injected with BrdU (50 μg/g body weight) twice a day (9 a.m. and 4 p.m.) for 7 days, followed by a chase period of 10 days. Representative pictures are shown (20×). Scale bar, 75 μm.

(legend continued on next page)

that BrdU-positive cells also express other putative stem cell markers, such as β1- and β4-integrins (Pajoohesh-Ganji et al., 2006), NGF (Li et al., 2017), ABCB5 (Ksander et al., 2014), and p63 (Lee et al., 2018).

In this study, we used two widely recognized markers, BrdU-label retention and p63, to identify corneal epithelial stem cells. In addition, we quantified the expression of ABCB5.

Because not every slow-cycling (BrdU$^+$) cell nor all p63-positive cells are epithelial stem cells, we quantified epithelial stem cells by colocalization of both markers: BrdU, located in most parts of the nucleus (Pajoohesh-Ganji et al., 2006), and p63. This method, which uses the slow-cycling characteristic of stem cells in combination with another putative marker, has been previously shown to reproducibly quantify epithelial stem cells in mice (Pajoohesh-Ganji et al., 2006). Our data suggest that the SP/NK1R pathway has a role in stem cell exhaustion. In this vein, ablation of SP or its pharmacological inhibition preserves corneal epithelial stem cells, even when a very low amount of cells with a potential proliferative capacity is left after de-epithelization. As a consequence, a dramatic improvement of clinical signs of LSCD was observed. Interestingly, we showed for the first time that NK1R is expressed on the cell membrane of corneal epithelial stem cells, supporting the key role of SP (and nerves) in stem cell pathophysiology.

It should be noted that previous studies suggest a role for SP in promoting wound healing in the cornea (Nagano et al., 2003; Nakamura et al., 1997; Yang et al., 2014), although the specific effect of SP on epithelial stem cells was not studied. In this vein, we did not observe delayed epithelial healing *in vivo*, either in cases of total or partial epithelial ablation, in the knockout animal model. In addition, it has been suggested that the effect of SP on epithelial wound closure is time and concentration dependent (Hong et al., 2009). Hence, it is reasonable to hypothesize that an early, controlled release of SP is beneficial, while excessive amounts may impair healing. A similar effect was observed on vascular endothelial cells, where proliferation was stimulated at low SP concentration but impaired at higher ones (Villablanca et al., 1994).

A potential mechanism inducing corneal epithelial senescence is mTOR signaling, which controls aging and lifespan by regulation of stem cell proliferation and differentiation in the oral and intestinal mucosa, skin, and cornea (Castilho et al., 2009; Gidfar et al., 2017; Iglesias-Bartolome et al., 2012; Weichhart, 2018).

Interestingly, the effects of mTOR activation are double faced, depending on duration. Short-term activation of mTOR is beneficial, since it increases cell proliferation (Saxton and Sabatini, 2017). Long-term activation, instead, leads to stem cell exhaustion, and its inhibition preserves adult stem cell function (Johnson et al., 2013). Interestingly, previous data of our group suggest that alkali burns—a common cause of LSCD—increase the expression of SP and leukocyte infiltration in the cornea (Barbariga et al., 2018a; Bignami et al., 2014), which could accelerate senescence and depletion of stem cells.

DNA damage is also a major cause of stem cell senescence and exhaustion in several tissues (Chitikova et al., 2014; Wang et al., 2012; Yu et al., 2015). In this vein, restraining mTOR activation suppresses cellular senescence in several tissues (Castilho et al., 2009; Demidenko et al., 2009; Iglesias-Bartolome et al., 2012), and specifically inhibits H2AX histone phosphorylation (Pospelova et al., 2009). In fact, phosphorylated H2AX (γH2AX) is an early marker of DNA damage; its phosphorylation follows genotoxic stress and plays an essential role in the recruitment of DNA repair proteins (Redon et al., 2002). Interestingly, γH2AX can persist over time when the DNA repair process is slow or inefficient or when cellular senescence takes place, leading to permanently unrepaired DNA (Siddiqui et al., 2015).

Our data show that the release of SP in the highly pro-inflammatory LSCD model induces mTOR expression and promotes cellular senescence through H2AX phosphorylation. In this vein, the previous finding that mTOR inhibition prolongs the survival of corneal epithelial cells *in vitro* and maintains their proliferative potential corroborates our results (Gidfar et al., 2017). In accordance, it has recently been reported that mTOR signaling inhibition accelerates corneal healing following alkali burn (Wang et al., 2020). Others (Park et al., 2019) have shown that the mTOR inhibitor rapamycin aggravates corneal LSCD by upregulating the inflammatory response. An explanation for this apparent discrepancy is that rapamycin almost completely inhibits mTOR by blocking substrate recruitment (Waldner et al., 2016), which results in an imbalanced pro-inflammatory environment, detrimental to stem cell function (Park et al., 2019). We observed, instead, that SP ablation promotes a partial inhibition of mTOR activity (around 50%), which results in beneficial effects on epithelial cell survival and proliferation.

LSCD is a major clinical problem and an area of unmet medical need. While cell transplantation therapies are

---

(B) Colocalization between p63 and BrdU was performed. Representative pictures of colocalization points are shown in magenta (20×). Scale bar, 75 μm. Stem cell-like cells were identified when the colocalized points represented more than 50% of the nucleus, using DAPI as a reference (white arrowheads).
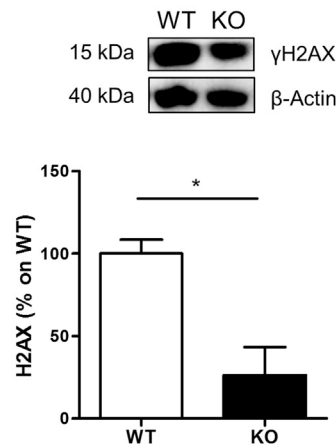
(C) Neurokinin-1 receptor, BrdU, and p63 triple staining. Representative pictures are shown (40×). Scale bar, 25 μm. Graphs show mean values ±SEM (n = 5 mice/group); statistical analysis by one-way ANOVA followed by Tukey's test: *p < 0.05, **p < 0.01, ***p < 0.001.

A
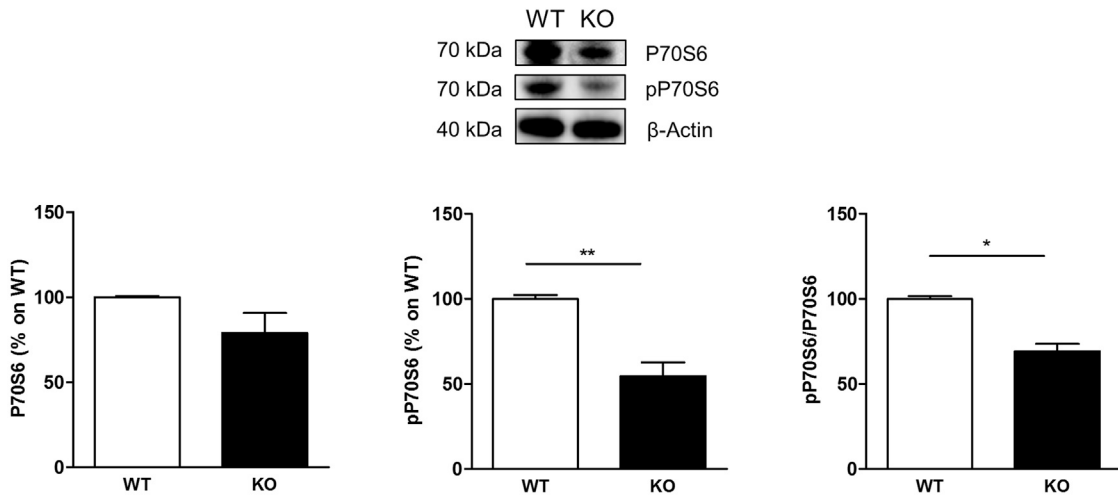
B

Figure 6. SP ablation results in decreased mTOR signaling and senescence in corneal epithelium
(A) Expression of P70S6 and pP70S6, downstream proteins in mTOR pathway, evaluated by western blot. A representative blot is shown. A ratio between pP70S6 and P70S6 expression was performed in order to determine mTOR pathway activation.
(B) Expression of γH2AX as a senescence marker. A representative blot is shown. Graphs show mean values ±SEM (n = 4 mice/group); statistical analysis by unpaired Student's t test: *p < 0.05.

now available, they cannot be accessed by everyone in need, and chronic inflammation significantly impairs their efficacy. Our data suggest that expression of SP can induce senescence and exhaustion of residual stem cells through activation of NK1R. In summary, we suggest that inhibition of SP activity by means of topical NK1R antagonists represents an attractive option to treat LSCD. We anticipate that our findings have relevant translational

implications, because clinically available NK1R antagonists can be repurposed for ocular use.

EXPERIMENTAL PROCEDURES

Stem cell deficiency model
Eight-week-old male mice C57BL6/N (Charles River, Calco, Italy) (WT mice, n = 30) and Tac1-deficient B6.Cg-Tac1tm1Bbm/J

(Jackson Laboratories, Bar Harbor, ME, USA) (TAC1-KO mice, n = 18) were used in all experiments. TAC1-KO mice are homozygous null for the TAC1 gene (C57BL6/N background), which encodes SP. They are viable, fertile, normal in size, and do not display any gross physical or behavioral abnormalities. In previous work, we showed that TAC1-KO mice did not present ocular abnormalities. The corneal thickness and transparency as well as the corneal nerve length are similar to C57BL/6 mice (Barbariga et al., 2018b).

Each animal was anesthetized with an intraperitoneal injection of tribromoethanol (250 mg/kg) and a topical anesthetic was applied to their ocular surface prior to the surgical procedure. Total de-epithelization was performed based on the model previously described (Amirjamshidi et al., 2011), using a blunt spatula to scrape the entire corneal epithelium, including the limbus. Then, fluorescein staining was used to confirm complete removal of the corneal epithelium under the blue light of a slit-lamp microscope. After wounding, eyes were treated with ophthalmic moxifloxacin once a day for 1 week to minimize inflammation. Fourteen days after de-epithelization, mice were euthanized using carbon dioxide inhalation and subsequent cervical dislocation. Corneas were collected for immunostaining and western blot analysis. A group of animals (n = 5) was followed up to 4 weeks in order to evaluate our stem cell deficiency experimental model stability. All experimental protocols were approved by the Animal Care and Use Committee of the Istituto di Ricovero e cura a Carattere Scientifico San Raffaele Scientific Institute, in accordance with the ARVO Statement for the Use of Animals in Ophthalmic and Vision Research.

Fosaprepitant treatment

To evaluate the pharmacological inhibition of SP, mice topically received 10 μL of fosaprepitant (IVEMEND, Merck Sharp & Dohme Ltd., Hoddesdon, UK) in two different concentrations: FOSA 0.1 (n = 5) or FOSA 1 (n = 5) four times a day every 2 h for 16 days. Control animals received instead 10 μL of vehicle (PBS) (WT, n = 5). The treatments started the same day that corneal de-epithelization was performed.

Corneal opacity and wound healing

Every day after de-epithelization, *in vivo* corneal photographs were taken using a digital camera (EOS30D; Canon, Tokyo, Japan) attached to a slit-lamp microscope (Photoslitmap 40 SL-P; Zeiss, Oberkochen, Germany) to assess corneal condition. Corneal opacity was evaluated using a grading score (from 0 to 4; 0 = completely clear, 4 = completely opaque) as previously described (Yoeruek et al., 2010). Additionally, *in vivo* corneal fluorescein staining was used to evaluate wound closure. Eyes were photographed under blue light (with or without a yellow filter) of the slit-lamp microscope. The percentage of green fluorescent area on the total corneal area was evaluated by analyzing images by ImageJ software (National Institutes of Health, Bethesda, MD, USA).

Goblet cell identification

To identify the presence of goblet cells, PAS staining was performed following the same experimental protocol previously described (Ferrari et al., 2013). The number of PAS⁺ cells was quantified in

at least 15 sections per individual sample. The results were expressed as PAS⁺ cells per section.

In addition, mucin 5AC (Muc5AC) immunofluorescence was performed. Briefly, eyes were removed and carefully embedded in the same orientation in optimal cutting temperature medium (OCTKillik; Bio-Optica, Milan, Italy), and 8-μm cryosections were performed. After fixation in 4% paraformaldehyde (Sigma-Aldrich, St. Louis, MO, USA) for 15 min, the sections were permeabilized using 0.1% Triton for 10 min and then blocked with 2% BSA in PBS for 1 h at room temperature (RT). The immunostaining was performed using mouse anti-Muc5AC (1/100, MA5-12178, Invitrogen) overnight at 4°C. Secondary detection was performed using Alexa Fluor 546 donkey anti-mouse immunoglobulin (Ig) G (H + L) (1/1,000, A10036, Life Technologies) for 1 h at RT. Samples were counterstained with 4,6-diamidino-2-phenylindole (DAPI; Vector Laboratories, Burlingame, CA, USA), mounted, and photographed by epifluorescence microscope (Leica CTR5500; Leica Microsystems, Wetzlar, Germany) (20×). An isotype control was used to establish a fluorescence threshold (Figure S4). Muc5AC⁺ cells were quantified in at least 15 sections per individual sample. The results were expressed as Muc5AC⁺ cells per section.

Conjunctival and corneal epithelial cell identification

The presence of conjunctival or corneal epithelial cells was evaluated by immunofluorescence as previously described in the section "goblet cell identification." The immunostaining was performed using rat anti-cytokeratin-19 (CK19) (1/300, MABT913, Millipore), rabbit anti-cytokeratin-13 (CK13) (1/100, SN71-09, Invitrogen), rabbit anti-cytokeratin-8 (CK8) (1/200, AB59400, Abcam), and guinea pig anti-cytokeratin-12 (CK12) (1/100, AP09545SU-N, Origene) for 1 h at RT. Secondary detection was performed using Alexa Fluor 594 donkey anti-rabbit IgG (1/1,000, A21207, Life Technologies), Alexa Fluor 594 donkey anti-rat (1/1,000, A21209, Life Technologies), and Alexa Fluor 488 donkey anti-guinea pig (1/1,000, A11073, Life Technologies) for 1 h at RT, diluted in blocking solution. The image analysis was performed using ImageJ software (National Institutes of Health, Bethesda, MD, USA). An isotype control was used to establish a fluorescence threshold (Figure S4). Then, the expression of the cytokeratins was quantified in terms of the percentage of positive area (% area) in the epithelium in at least 15 sections per individual sample.

Stem cell-like cells detection

Immediately after corneal dispithelization, animals were intraperitoneally injected with BrdU (50 μg/g body weight, ab142567, Abcam) twice a day (9 a.m. and 4 p.m.) for 7 days. At the indicated time points, eyes were processed for immunostaining as previously described in the section "goblet cell identification." After a 10-min fixation with 4% paraformaldehyde on ice, samples were boiled in 10 mM citrate buffer (pH = 6.00) in the microwave (700 W) for 4 min. After cooling down to RT, samples were incubated with a blocking solution (2% BSA, 0.1 Triton X-100, 10% normal donkey serum in PBS) for 1 h at RT. Primary detection was performed with rabbit anti-p63 (1/300, ab124762, Abcam) for 1 h at RT, followed by Alexa Fluor 488 donkey anti-rabbit (1/1,000, A21206, Life Technologies) secondary antibody for 1 h at RT. A second fixation was

performed with 4% paraformaldehyde during 20 min on ice and then transferred to 2 N HCl at 37°C for 15 min followed by a neutralization step with borate buffer (pH = 8.50) for 8 min. Samples were immersed again in blocking solution for 30 min and then incubated overnight with rat anti-BrdU (1/100, ab6326, Abcam) primary antibody at 4°C, followed by Alexa Fluor 594 donkey anti-rat (1/1,000, A21209, Life Technologies) for 1 h at RT. Finally, sections were mounted with Vector Shield mounting medium (Vector Laboratories, Burlingame, CA) containing DAPI. The images were acquired by epifluorescence microscope (Leica CTR5500; Leica Microsystems, Wetzlar, Germany) (20×) and analyzed with ImageJ software. An isotype control was used to establish a fluorescence threshold (Figure S4). Then, the % area for each marker was quantified in the epithelium. Colocalization between p63 and BrdU was assessed using the colocalization plug-in (National Institutes of Health, Bethesda, MD, USA), and then quantified as percentage of colocalized points (shown in magenta). Then, stem cell-like cells were identified and quantified according to the score described by Pajoohesh-Ganji et al. (2006). A cell with more than 50% of the nucleus positive for both p63 and BrdU was considered a stem cell-like cell (Figure S5).

NK1R expression

To evaluate whether the NK1R was expressed by epithelial stem cell-like cells, we performed a triple staining using p63 and BrdU as previously described earlier. Primary goat anti-NKR1 (1/800, ab61705, Abcam) was co-incubated with p63 antibody for 1 h at RT, followed by Alexa Fluor 633 donkey anti-goat (1/1,000, A21082, Life Technologies) for 1 h at RT. Pictures were acquired in a DeltaVision Ultra microscope (GE healthcare, Chicago, IL, USA) (40×) and image analysis was performed using ImageJ software (National Institutes of Health, Bethesda, MD, USA). An isotype control was used to establish a fluorescence threshold (Figure S4). Colocalization analysis was performed as described above.

Expression of proteins related to the mTOR signaling pathway

The expression of p70S6 kinase (P70S6), phospho-p70 S6 kinase (pP70S6), and phospho-histone 2-AX (γH2AX) was evaluated by western blot. After corneal dissection, corneal epithelium was isolated after 30 min of EDTA treatment (Sigma-Aldrich, St. Louis, MO, USA) at 37°C and re-suspended RIPA Buffer (Sigma-Aldrich) containing protease inhibitor. A pool of four corneal epithelia from different animals was used (WT, n = 8; TAC1-KO, n = 12). A sample of 10 μg of proteins from WT or TAC1-KO epithelia was resolved on NuPAGE4–12% Bis-Tris Protein Gels (Thermo Fisher) and electro-transferred to nitrocellulose membranes (Amersham, Little Chalfont, UK). Red Ponceau staining (Sigma-Aldrich) was used to evaluate protein transfer. Membranes were blocked in a Tris-buffered solution (TBS) 3% BSA, 0.1% Tween 20 for 1 h at RT. The following primary antibodies were used: rabbit anti-P70S6 (1/1,000, 9202, Cell Signaling), mouse anti-pP70S6(1/1,000, 9206, Cell Signaling), and rabbit anti-γH2AX (1/1,000, NB100-384, Novus Biologicals), followed by anti-mouse or antirabbit-HRP-conjugated secondary antibodies (1/5,000, NA9310V and NA9340V respectively, GE Healthcare). As loading control, expression of β-actin HRP-conjugated mouse monoclonal antibody (1/

1,000, A3854, Merck) was used. Bands were identified based on molecular weight using the protein marker (Precision Plus Protein Dual Color Standards, 1610374, Bio-Rad) as a reference. Intensities were quantified using ImageJ software (National Institutes of Health, Bethesda, MD, USA).

Statistical analysis

Statistical calculation was performed using GraphPad Prism 5.0 software (GraphPad Software, La Jolla, CA, USA). Data were expressed as mean ± standard error of mean (SEM).The statistical significance of the differences between the two groups was calculated by unpaired Student's t test,α = 0.05. When three experimental groups were compared, one-way ANOVA followed by Tukey's *post hoc* test (α = 0.05) was used. For corneal wound closure and corneal opacity analysis, two-way ANOVA was performed, considering $p < 0.05$ statistically significant.

SUPPLEMENTAL INFORMATION

Supplemental information can be found online at https://doi.org/10.1016/j.stemcr.2022.02.012.

AUTHOR CONTRIBUTIONS

R.L.V., conception and design, collection and/or assembly of data, data analysis and interpretation, and manuscript writing; F.T., collection and/or assembly of data and data analysis; M.B., collection and/or assembly of data and data analysis and interpretation; P.F., collection and/or assembly of data and data analysis and interpretation; P.R., financial support and final approval of manuscript; G.F., conception and design, data analysis and interpretation, manuscript writing, financial support, and final approval of manuscript.

CONFLICTS OF INTEREST

G.F. and P.R. are inventors of a patent involving fosaprepitant. The other authors declare no competing interests.

ACKNOWLEDGMENTS

REFERENCES

Ahmad, S. (2012). Concise review: limbal stem cell deficiency, dysfunction, and distress. Stem Cells Transl. Med. *1*, 110–115.

Amirjamshidi, H., Milani, B.Y., Sagha, H.M., Movahedan, A., Shafiq, M.A., Lavker, R.M., Yue, B.Y.T., and Djalilian, A.R. (2011). Limbal fibroblast conditioned media: a non-invasive treatment for limbal stem cell deficiency. Mol. Vis. *17*, 658–666.

Amitai-Lange, A., Altshuler, A., Bubley, J., Dbayat, N., Tiosano, B., and Shalom-Feuerstein, R. (2015). Lineage tracing of stem and progenitor cells of the murine corneal epithelium. Stem Cells *33*, 230–239.

Atallah, M.R., Palioura, S., Perez, V.L., and Amescua, G. (2016). Limbal stem cell transplantation: current perspectives. Clin. Ophthalmol. *10*, 593–602.

Barbariga, M., Fonteyne, P., Ostadreza, M., Bignami, F., Rama, P., and Ferrari, G. (2018a). Substance p modulation of human and murine corneal neovascularization. Investig. Ophthalmol. Vis. Sci. *59*, 1305–1312.

Barbariga, M., Rabiolo, A., Fonteyne, P., Bignami, F., Rama, P., and Ferrari, G. (2018b). The effect of aging on nerve morphology and substance P expression in mouse and human corneas. Investig. Ophthalmol. Vis. Sci. *59*, 5329–5335.

Baylis, O., Figueiredo, F., Henein, C., Lako, M., and Ahmad, S. (2011). 13 years of cultured limbal epithelial cell therapy: a review of the outcomes. J. Cell. Biochem. *112*, 993–1002.

Bignami, F., Giacomini, C., Lorusso, A., Aramini, A., Rama, P., and Ferrari, G. (2014). NK1 receptor antagonists as a new treatment for corneal neovascularization. Invest. Ophthalmol. Vis. Sci. *55*, 6783–6794.

Bignami, F., Lorusso, A., Rama, P., and Ferrari, G. (2017). Growth inhibition of formed corneal neovascularization following Fosaprepitant treatment. Acta Ophthalmol. *95*, e641–e648.

Castilho, R.M., Squarize, C.H., Chodosh, L.A., Williams, B.O., and Gutkind, J.S. (2009). mTOR mediates Wnt-induced epidermal stem cell exhaustion and aging. Cell Stem Cell *5*, 279–289.

Chitikova, Z.V., Gordeev, S.A., Bykova, T.V., Zubova, S.G., Pospelov, V.A., and Pospelova, T.V. (2014). Sustained activation of DNA damage response in irradiated apoptosis-resistant cells induces reversible senescence associated with mTOR downregulation and expression of stem cell markers. Cell Cycle *13*, 1424–1439.

Cotsarelis, G., Cheng, S.Z., Dong, G., Sun, T.T., and Lavker, R.M. (1989). Existence of slow-cycling limbal epithelial basal cells that can be preferentially stimulated to proliferate: implications on epithelial stem cells. Cell *57*, 201–209.

Daniels, J.T., Dart, J.K.G., Tuft, S.J., and Khaw, P.T. (2001). Corneal stem cells in review. Wound Repair Regen. *9*, 483–494.

Daniels, J.T., Harris, A.R., and Mason, C. (2006). Corneal epithelial stem cells in health and disease. Stem Cell Rev. *2*, 247–254.

Demidenko, Z.N., Zubova, S.G., Bukreeva, E.I., Pospelov, V.A., Pospelova, T.V., and Blagosklonny, M.V. (2009). Rapamycin decelerates cellular senescence. Cell Cycle *8*, 1888–1895.

Doles, J., Storer, M., Cozzuto, L., Roma, G., and Keyes, W.M. (2012). Age-associated inflammation inhibits epidermal stem cell function. Genes Dev. *26*, 2144–2153.

Dua, H.S., and Azuara-Blanco, A. (2000). Limbal stem cells of the corneal epithelium. Surv. Ophthalmol. *44*, 415–425.

Dua, H.S., Saini, J.S., Azuara-Blanco, A., and Gupta, P. (2000). Limbal stem cell deficiency: concept, aetiology, clinical presentation, diagnosis and management. Indian J. Ophthalmol. *48*, 83–92.

Ferrari, G., Bignami, F., Giacomini, C., Franchini, S., and Rama, P. (2013). Safety and efficacy of topical infliximab in a mouse model of ocular surface scarring. Investig. Ophthalmol. Vis. Sci. *54*, 1680–1688.

Gidfar, S., Milani, F.Y., Milani, B.Y., Shen, X., Eslani, M., Putra, I., Huvard, M.J., Sagha, H., and Djalilian, A.R. (2017). Rapamycin pro-

longs the survival of corneal epithelial cells in culture. Sci. Rep. *7*, 40308.

Di Girolamo, N., Bobba, S., Raviraj, V., Delic, N.C., Slapetova, I., Nicovich, P.R., Halliday, G.M., Wakefield, D., Whan, R., and Lyons, J.G. (2015). Tracing the fate of limbal epithelial progenitor cells in the murine cornea. Stem Cells *33*, 157–169.

Glass, C.K., Saijo, K., Winner, B., Marchetto, M.C., and Gage, F.H. (2010). Mechanisms underlying inflammation in neurodegeneration. Cell *140*, 918–934.

Guo, Z.H., Zhang, W., Jia, Y.Y.S., Liu, Q.X., Li, Z.F., and Lin, J.S. (2018). An insight into the difficulties in the discovery of specific biomarkers of limbal stem cells. Int. J. Mol. Sci. *19*, 1982.

Hatch, K.M., and Dana, R. (2009). The structure and function of the limbal stem cell and the disease states associated with limbal stem cell deficiency. Int. Ophthalmol. Clin. *49*, 43–52.

Hong, H.S., Lee, J., Lee, E., Kwon, Y.S., Lee, E., Ahn, W., Jiang, M.H., Kim, J.C., and Son, Y. (2009). A new role of substance P as an injury-inducible messenger for mobilization of CD29 + stromal-like cells. Nat. Med. *15*, 425–435.

Iglesias-Bartolome, R., Patel, V., Cotrim, A., Leelahavanichkul, K., Molinolo, A.A., Mitchell, J.B., and Gutkind, J.S. (2012). mTOR inhibition prevents epithelial stem cell senescence and protects from radiation-induced mucositis. Cell Stem Cell *11*, 401–414.

Johnson, S.C., Rabinovitch, P.S., and Kaeberlein, M. (2013). MTOR is a key modulator of ageing and age-related disease. Nature *493*, 338–345.

King, K.Y., and Goodell, M.A. (2011). Inflammatory modulation of HSCs: viewing the HSC as a foundation for the immune response. Nat. Rev. Immunol. *11*, 685–692.

Kizil, C., Kyritsis, N., and Brand, M. (2015). Effects of inflammation on stem cells: together they strive? EMBO Rep. *16*, 416–426.

Ksander, B.R., Kolovou, P.E., Wilson, B.J., Saab, K.R., Guo, Q., Ma, J., McGuire, S.P., Gregory, M.S., Vincent, W.J.B., Perez, V.L., et al. (2014). ABCB5 is a limbal stem cell gene required for corneal development and repair. Nature *511*, 353–357.

Lasagni Vitar, R.M., Barbariga, M., Fonteyne, P., Bignami, F., Rama, P., and Ferrari, G. (2021). Modulating ocular surface pain through neurokinin-1 receptor blockade. Investig. Ophthalmol. Vis. Sci. *62*, 26.

Lee, H.K., Ryu, J.S., Jeong, H.J., Kim, M.K., and Oh, J.Y. (2018). Protection of corneal limbus from riboflavin prevents epithelial stem cell loss after collagen cross-linking. J. Ophthalmol. *2018*, 6854298.

Li, F.X.Z., Xu, F., Lin, X., Wu, F., Zhong, J.Y., Wang, Y., Guo, B., Zheng, M.H., Shan, S.K., and Yuan, L.Q. (2020). The role of substance P in the regulation of bone and cartilage metabolic activity. Front. Endocrinol. (Lausanne). *11*, 77.

Li, J., Xiao, Y., Coursey, T.G., Chen, X., Deng, R., Lu, F., Pflugfelder, S.C., and Li, D.Q. (2017). Identification for differential localization of putative corneal epithelial stem cells in mouse and human. Sci. Rep. *7*, 5169.

Ljubimov, A.V., and Saghizadeh, M. (2015). Progress in corneal wound healing. Prog. Retin. Eye Res. *49*, 17–45.

Magnuson, B., Ekim, B., and Fingar, D.C. (2012). Regulation and function of ribosomal protein S6 kinase (S6K) within mTOR signalling networks. Biochem. J. *441*, 1–21.

Mashaghi, A., Marmalidou, A., Tehrani, M., Grace, P.M., Pothoulakis, C., and Dana, R. (2016). Neuropeptide substance P and the immune response. Cell. Mol. Life Sci. *73*, 4249–4264.

Meyer-Blazejewska, E.A., Call, M.K., Yamanaka, O., Liu, H., Schlötzer-Schrehardt, U., Kruse, F.E., and Kao, W.W. (2011). From hair to cornea: toward the therapeutic use of hair follicle-derived stem cells in the treatment of limbal stem cell deficiency. Stem Cells *29*, 57–66.

Muñoz, M., and Coveñas, R. (2014). Involvement of substance P and the NK-1 receptor in human pathology. Amino Acids *46*, 1727–1750.

Nagano, T., Nakamura, M., Nakata, K., Yamaguchi, T., Takase, K., Okahara, A., Ikuse, T., and Nishida, T. (2003). Effects of substance P and IGF-1 in corneal epithelial barrier function and wound healing in a rat model of neurotrophic keratopathy. Invest. Ophthalmol. Vis. Sci. *44*, 3810–3815.

Nakamura, M., Ofuji, K., Chikama, T.I., and Nishida, T. (1997). Combined effects of substance P and insulin-like growth factor-1 on corneal epithelial wound closure of rabbit in vivo. Curr. Eye Res. *16*, 275–278.

Nowicki, M., Ostalska-Nowicka, D., Kondraciuk, B., and Miskowiak, B. (2007). The significance of substance P in physiological and malignant haematopoiesis. J. Clin. Pathol. *60*, 749–755.

Pajoohesh-Ganji, A., Pal-Ghosh, S., Simmens, S.J., and Stepp, M.A. (2006). Integrins in slow-cycling corneal epithelial cells at the limbus in the mouse. Stem Cells *24*, 1075–1086.

Pajoohesh-Ganji, A., Pal-Ghosh, S., Tadvalkar, G., and Stepp, M.A. (2012). Corneal goblet cells and their niche: implications for corneal stem cell deficiency. Stem Cells *30*, 2032–2043.

Pal-Ghosh, S., Tadvalkar, G., Jurjus, R.A., Zieske, J.D., and Stepp, M.A. (2008). BALB/c and C57BL6 mouse strains vary in their ability to heal corneal epithelial debridement wounds. Exp. Eye Res. *87*, 478–486.

Park, J.W., Ko, J.H., Kim, B.H., Ryu, J.S., Kim, H.J., Kim, M.K., and Oh, J.Y. (2019). Inhibition of mTOR by rapamycin aggravates corneal epithelial stem cell deficiency by upregulating inflammatory response. Stem Cells *37*, 1212–1222.

Pellegrini, G., Dellambra, E., Golisano, O., Martinelli, E., Fantozzi, I., Bondanza, S., Ponzin, D., McKeon, F., and De Luca, M. (2001). p63 identifies keratinocyte stem cells. Proc. Natl. Acad. Sci. U S A. *98*, 3156–3161.

Pluchino, S., Muzio, L., Imitola, J., Deleidi, M., Alfaro-Cervello, C., Salani, G., Porcheri, C., Brambilla, E., Cavasinni, F., Bergamaschi, A., et al. (2008). Persistent inflammation alters the function of the endogenous brain stem cell compartment. Brain *131*, 2564–2578.

Pospelova, T.V., Demidenko, Z.N., Bukreeva, E.I., Pospelov, V.A., Gudkov, A.V., and Blagosklonny, M.V. (2009). Pseudo-DNA damage response in senescent cells. Cell Cycle *8*, 4112–4118.

Rama, P., Matuska, S., Paganoni, G., Spinelli, A., De Luca, M., and Pellegrini, G. (2010). Limbal stem-cell therapy and long-term corneal regeneration. N. Engl. J. Med. *363*, 147–155.

Rama, P., Ferrari, G., and Pellegrini, G. (2017). Cultivated limbal epithelial transplantation. Curr. Opin. Ophthalmol. *28*, 387–389.

Redon, C., Pilch, D., Rogakou, E., Sedelnikova, O., Newrock, K., and Bonner, W. (2002). Histone H2A variants H2AX and H2AZ. Curr. Opin. Genet. Dev. *12*, 162–169.

Russell, R.C., Fang, C., and Guan, K.L. (2011). An emerging role for TOR signaling in mammalian tissue and stem cell physiology. Development *138*, 3343–3356.

Sacchetti, M., Rama, P., Bruscolini, A., and Lambiase, A. (2018). Limbal stem cell transplantation: clinical results, limits, and perspectives. Stem Cells Int. *2018*, 8086269.

Sangwan, V.S., Basu, S., Vemuganti, G.K., Sejpal, K., Subramaniam, S.V., Bandyopadhyay, S., Krishnaiah, S., Gaddipati, S., Tiwari, S., and Balasubramanian, D. (2011). Clinical outcomes of xeno-free autologous cultivated limbal epithelial transplantation: a 10-year study. Br. J. Ophthalmol. *95*, 1525–1529.

Sartaj, R., Zhang, C., Wan, P., Pasha, Z., Guaiquil, V., Liu, A., Liu, J., Luo, Y., Fuchs, E., and Rosenblatt, M.I. (2017). Characterization of slow cycling corneal limbal epithelial cells identifies putative stem cell markers. Sci. Rep. *7*, 1–14.

Saxton, R.A., and Sabatini, D.M. (2017). mTOR signaling in growth, metabolism, and disease. Cell *168*, 960–976.

Shaheen, B.S., Bakir, M., and Jain, S. (2014). Corneal nerves in health and disease. Surv. Ophthalmol. *59*, 263–285.

Siddiqui, M.S., François, M., Fenech, M.F., and Leifert, W.R. (2015). Persistent γH2AX: a promising molecular marker of DNA damage and aging. Mutat. Res. Rev. Mutat. Res. *766*, 1–19.

Suvas, S. (2017). Role of substance P neuropeptide in inflammation, wound healing, and tissue homeostasis. J. Immunol. *199*, 1543–1552.

Villablanca, A.C., Murphy, C.J., and Reid, T.W. (1994). Growth-promoting effects of substance P on endothelial cells in vitro: synergism with calcitonin gene-related peptide, insulin, and plasma factors. Circ. Res. *75*, 1113–1120.

Waldner, M., Fantus, D., Solari, M., and Thomson, A.W. (2016). New perspectives on mTOR inhibitors (rapamycin, rapalogs and TORKinibs) in transplantation. Br. J. Clin. Pharmacol. *82*, 1158–1170.

Wang, J., Sun, Q., Morita, Y., Jiang, H., Groß, A., Lechel, A., Hildner, K., Guachalla, L.M., Gompf, A., Hartmann, D., et al. (2012). A differentiation checkpoint limits hematopoietic stem cell self-renewal in response to DNA damage. Cell *148*, 1001–1014.

Wang, Y., Gao, G., Wu, Y., Wang, Y., Wu, X., and Zhou, Q. (2020). S100A4 silencing facilitates corneal wound healing after alkali burns by promoting autophagy via blocking the PI3K/Akt/mTOR signaling pathway. Invest. Ophthalmol. Vis. Sci. *61*, 19.

Watanabe, M., Nakayasu, K., Iwatsu, M., and Kanai, A. (2002). Endogenous substance P in corneal epithelial cells and keratocytes. Jpn. J. Ophthalmol. *46*, 616–620.

Weichhart, T. (2018). mTOR as regulator of lifespan, aging, and cellular senescence: a mini-review. Gerontology *64*, 127–134.

West, J.D. (2015). Evaluating alternative stem cell hypotheses for adult corneal epithelial maintenance. World J. Stem Cells *7*, 281.

Yang, L., Di, G., Qi, X., Qu, M., Wang, Y., Duan, H., Danielson, P., Xie, L., and Zhou, Q. (2014). Substance P promotes diabetic corneal epithelial wound healing through molecular mechanisms mediated via the neurokinin-1 receptor. Diabetes *63*, 4262–4274.

Yoeruek, E., Deuter, C., Gieselmann, S., Saygili, O., Spitzer, M.S., Tatar, O., Bartz-Schmidt, K.U., and Szurman, P. (2010). Long-term visual acuity and its predictors after cataract surgery in patients with uveitis. Eur. J. Ophthalmol. *20*, 694–701.

Yu, Q., Katlinskaya, Y.V., Carbone, C.J., Zhao, B., Katlinski, K.V., Zheng, H., Guha, M., Li, N., Chen, Q., Yang, T., et al. (2015). DNA-Damage-Induced type I interferon promotes senescence and inhibits stem cell function. Cell Rep. *11*, 785–797.

Ziche, M., Morbidelli, L., Pacini, M., Geppetti, P., Alessandri, G., and Maggi, C.A. (1990). Substance P stimulates neovascularization in vivo and proliferation of cultured endothelial cells. Microvasc. Res. *40*, 264–278.